https://doi.org/10.65646/3c p3es20dpi5b022

Waste-Derived Nitrogen-Doped Biochar for Persulfate Activation and Bisphenol A Degradation

K.A.S.S. Imbulana
Department of physical Sciences and technology
Faculty of Applied Sciences,
Sabaragamuwa University of Sri Lanka,
70140, Belihuloya, Sri Lanka
sandeepanisewmini2000@gmail.com

Chathumi Manangodage
Ecosphere Resilience Research Centre,
Faculty of Applied Sciences,
University of Sri Jayewardenepura,
10250, Nugegoda, Sri Lanka
chathumishanalika@sci.sjp.ac.lk

H. S. M. Soysa
Department of Physical Sciences and Technology
Faculty of Applied Sciences
Sabaragamuwa University of Sri Lanka
70140, *Belihuloya, Sri Lanka*
sasimali@appsc.sab.ac.lk

K.S.D. Premarathna
Ecosphere Resilience Research Centre,
Faculty of Applied Sciences,
University of Sri Jayewardenepura,
10250, Nugegoda, Sri Lanka
shashi8793@gmail.com

Anushka Upamali Rajapaksha
Ecosphere Resilience Research Centre,
Faculty of Applied Sciences,
University of Sri Jayewardenepura,
10250, Nugegoda, Sri Lanka
anurajapaksha@sjp.ac.lk

Meththika Vithanage
Department of Geochemistry,
Geological Survey of Denmark and Greenland,
1350, Copenhagen, Denmark
metvi@geus.dk

Abstract **- Plastic waste constitutes a major environmental concern within municipal solid waste management systems. Its progressive degradation and weathering facilitate the leaching of hazardous additives, notably bisphenol A (BPA), a well-documented endocrine-disrupting compound with significant toxicological effects for aquatic ecosystems and human health. The aim of this study was to use municipal solid waste (MSW) compost residue biomass, including coconut shell, coconut husk, and wood fractions, to prepare nitrogen-doped biochar (N-MSW-BC) for persulfate (PS)-mediated catalytic degradation of BPA. The biomass was pyrolyzed in the presence of urea and sodium bicarbonate. The physicochemical properties of N-MSW-BC were assessed using proximate analysis, point of zero charge (pH_{pzc}), and Fourier transform infrared (FTIR) spectroscopy. The potential of BPA degradation by N-MSW-BC was evaluated through adsorption experiments, pre-adsorption kinetics, and synchronous degradation studies. FTIR verified the integration of nitrogen-containing heterocycles into the carbon matrix, which showed distinctive bands near 3660–3280 cm^{-1} (O-H/N-H stretching) and at 1594 cm^{-1}, attributed to overlapping aromatic C=C and C=N stretching and N-H bending vibrations. A stable carbon content of 41.83% was determined by proximate analysis, suggesting a graphitic-rich carbon matrix ideal for PS activation. BPA removal remained consistently high (~99.7%) across a pH range of 2-9 in a pH-edge experiment with the N-MSW-BC persulfate (10 mM) system. At 180 min, pre-adsorption followed by PS activation achieved 99.5% BPA elimination; whereas, the synchronous system only achieved 90.5% within the same exposure period. The electrostatic forces with BPA and biochar were influenced by their pH_{pzc} (~ 8.2). These findings suggest an interfacial, adsorption-mediated catalytic process, establishing N-MSW-BC generated from compost residues as a sustainable material for BPA remediation by persulfate activation.**

Keywords: *Advanced oxidation, Biochar, Municipal solid waste valorization*

I. INTRODUCTION

Bisphenol A (BPA) has been widely released into aqueous systems, including landfill leachate, industrial

effluents, and municipal wastewater, due to the explosive growth of the chemical and plastics industries [1]. It mimics natural hormones and disrupts reproductive and developmental systems even at trace levels, BPA is a persistent phenolic endocrine disruptor that poses serious dangers to aquatic life and human health [1]. BPA tends to persist in the environment for long periods, accumulating in sediments and biological tissues because it is hydrophobic, chemically stable, and resistant to traditional biological treatment methods [2]. The recalcitrance of BPA prevents conventional wastewater treatment facilities from completely removing it, leading to residual concentrations that are released into natural water bodies [3]. The development of effective, economical, and environmentally friendly remediation solutions that can achieve complete degradation of BPA rather than only phase transfer is now desperately needed.

The sulfate radicals generated during persulfate (PS) activation have high oxidation potential. Therefore, PS-based advanced oxidation processes (PS-AOPs) have become one of the most promising remediation strategies for the degradation of persistent organic pollutants in the environment [1, 3]. Biochar prepared from forestry and agricultural biomass is found to efficiently activate PS via both radical and non-radical routes. Nitrogen (N) doping, which introduces catalytically active nitrogen species such as pyridinic, pyrrolic, and graphitic nitrogen, facilitating electron transfer and promoting PS decomposition, has been thoroughly investigated as a strategy to alter the electronic structure of the carbon matrix to further improve catalytic performance [1, 6]. For this purpose, a variety of nitrogen precursors, such as urea, melamine, and ammonium salts, have been used, often in conjunction with pore-forming or templating agents, such as KOH, $ZnCl_2$, or $NaHCO_3$, to increase porosity and surface area [1]. A different circular economy approach that addresses waste management issues is the valorization of biomass waste into biochar, which transforms low-value or wasted organic material into value-added catalytic materials [3].

Despite these advances, the biochar feedstocks most commonly employed in PS-based systems remain relatively homogeneous and well-characterized lignocellulosic residues, such as rice husk, sawdust, and algal biomass, while municipal solid waste (MSW) compost residues heterogeneous mixtures dominated by coconut shell, coconut husk, and wood fractions remain largely unexplored as precursors for nitrogen-doped (N-doped) biochar in PS-mediated degradation of BPA, despite the opportunity such valorization presents to simultaneously address a waste-management burden and generate a functional carbon material for organic micropollutant remediation; moreover, the adsorptive and PS-activation performance of N-doped biochar derived from such heterogeneous feedstock, and the extent to which treatment configuration governs BPA removal efficiency, have not been systematically established. A related gap concerns process design, as prior studies have generally evaluated adsorption and PS-mediated oxidation either simultaneously or as fully decoupled steps without direct comparison under equivalent conditions, leaving the mechanistic and kinetic consequences of pre-adsorbing BPA onto the biochar surface before PS activation relative to concurrent introduction of BPA and PS insufficiently clarified; pre-adsorption may locally enrich BPA concentration at the biochar water interface, potentially altering reactive-site availability, the dominant degradation pathway, and the resulting apparent kinetics, yet no study has directly compared pre-adsorption-assisted degradation against synchronous adsorption–degradation using an N-doped biochar derived specifically from MSW compost residue. Accordingly, this study investigates whether N-doped biochar derived from MSW compost residue can effectively adsorb BPA and facilitate PS-assisted degradation of BPA, and whether pre-adsorption confers a kinetic advantage over synchronous treatment due to interfacial concentration effects.

II. METHODOLOGY

A. Preparation of nitrogen-doped biochar

Nitrogen-doped biochar (N-MSW-BC) was synthesized from coconut shell, coconut husk, and wood as the biomass. Then, washed and oven-dried biomass was ground and mixed with $NaHCO_3$ (activating agent) and urea (nitrogen source) at a 1:1:1 mass ratio. Then, the biomass was pyrolyzed at 550 °C for 1.5 h under oxygen-limited conditions, and after natural cooling, the biochar was washed with distilled water. Then treated with 0.1 M HCl for 1 h to remove inorganic impurities, and repeatedly washed with ultrapure water until the filtrate reached near-neutral pH (7–8), yielding the final N-MSW-BC product.

B. Characterization of N-doped biochar

The moisture content of N-MSW-BC was determined via proximate analysis. The empty crucibles were weighed first without the lid, then with the lid, and finally with the N-MSW-BC. Subsequently, 1 g of N-MSW-BC was added to each crucible. The crucibles were heated to 105 °C at 7 °C/min for 3 h, with the lid open. The moisture content was calculated using Equation 1.

$$\textit{Moisture content}\,(\%) = \frac{(\textit{weight of sample} - \textit{weight of residue})}{\textit{weight of sample}} \times 100 \quad \textbf{(1)}$$

The crucibles used for moisture content determination were also used for volatile matter content determination. The crucibles were weighed and heated in the furnace to 450 °C at a heating rate of 7 °C/min for 2 h, with the lid closed. After combustion, the

crucibles with the samples were weighed. The volatile matter content was calculated using equation 2.

$$\text{Volatile matter content}(\%) = \frac{(\text{weight of sample} - \text{weight of residue})}{\text{weight of sample}} \times 100 \quad (2)$$

The crucibles that contained residue from the volatile matter content determination were used for ash content determination. The crucibles were weighed and heated in the furnace at 550 ℃ for 2 h with the lid open. After that, the crucibles were removed, and the weights were measured. The ash content was calculated using equation 3.

$$\textit{Ash content}(\%) = \frac{\textit{weight of residue}}{\textit{weight of sample}} \times 100 \quad (3)$$

The fixed carbon content was determined by subtracting the sum of moisture, volatile matter, and ash content from 100, as shown in equation 4.

$$\textit{Fixed Carbon Content} = 100 - (\textit{Moisture Content} + \textit{Volatile Matter} + \textit{Ash Content}) \quad (4)$$

Each experiment was performed in triplicate.

N-MSW-BC was subjected to Fourier Transform Infrared (FTIR) spectroscopy in order to identify their surface functional groups and confirm the addition of nitrogen-containing functional groups by nitrogen doping. FTIR analysis was performed in a range of 4000–450 cm^{-1}, and the resulting spectra were examined to identify the functional groups present in the biochar samples [9].

The zero-point charge of a material is the state in which the net charge on the N-MSW-BC surface is zero. The zero point charge (pHzpc) for the NBC samples was assessed using the pH drift method. Initially, 250.0 mL of a 0.01 M NaCl solution was prepared. A range of pH values was established at 2.0, 4.0, 6.0, 8.0, 10.0, and 12.0. The pH was adjusted from 2.0 using 0.1 M NaOH and HCl, and 25.0 mL samples were taken at each specified pH level. During this process, $N_{2(g)}$ was continuously purged to maintain the pH. Subsequently, 75.0 mg of the N-MSW-BC samples were added to each tube containing the 25 mL NaCl solution, and the mixtures were shaken for 24 h on a horizontal shaker. Afterwards, the final pH of each solution was recorded using the Adwa AD1030 bench meter. The pHzpc of the N-MSW-BC was determined by plotting the final pH values against the initial pH values of the solutions.

C. Batch Experiments

Batch degradation studies were conducted to determine the optimal pH and contact time for BPA degradation on N-MSW-BC. A stock solution of 250 mg L^{-1} was prepared by dissolving BPA (analytical reagent 99%) in acetonitrile (HPLC grade 99%). All the experiments were carried out at 25 °C. The concentration of BPA was detected by a High-Performance Liquid Chromatography (HPLC) system (Ultimate 3000, Thermo Scientific, USA) equipped with a Diode Array Detector (DAD) using a Hypersil GOLD C18 Selectivity LC Column (250 × 4.6 mm, particle size 5 µm. At a wavelength of 226 nm, BPA was detected using a mobile phase consisting of 100% acetonitrile and ultra-pure water in an initial ratio of 65: 35. The acetonitrile fraction was increased to 95% within 5 min, reduced to 80% between 6 and 7.5 min, and maintained at 95% from 7.5 to 20 min, while water was adjusted accordingly to maintain the gradient. The flow rate was set at 0.8–1.0 mL min^{-1} with an injection volume of 20 µL. The retention time of BPA under these conditions was 7.01 min. Calibration was performed using standard BPA solutions.

I. pH edge experiment

The pH-edge experiment used an Adwa AD1030 bench meter to change the pH between 2.0 and 9.0 using 0.1 M NaOH and HCl at a dosage of 1.0 g/L. Following pH adjustment, samples were equilibrated in a shaking water bath (150 rpm, 24 h) after being spiked with BPA and PS, along with a BPA-only control (no biochar). Sodium thiosulfate was used to quench the reactions, which were then filtered using PTFE syringe filters and analyzed by HPLC.

II. Kinetic experiments

N-MSW-BC (1.0 g/L) was hydrated overnight and then spiked with BPA to a final concentration of 20.0 mg/L to assess adsorption kinetics. Samples were collected at intervals of 2 to 1440 min, filtered through PTFE syringe filters, and then analyzed by HPLC. The equilibrium time was determined by plotting adsorption capacity versus contact time. A control experiment without N-MSW-BC was also performed under the same conditions.

III. Kinetics experiment for pre-adsorption experiment

The pre-adsorption experiment assessed the kinetics of BPA elimination when adsorption took place before oxidation. Before adding PS (10 mM), N-MSW-BC (1.0 g/L) was spiked with BPA (20.0 mg/L) and allowed to adsorb for 3 h. Samples were collected at intervals of 2 to 1440 min, filtered using PTFE syringe filters, quenched with sodium thiosulfate, and analyzed by HPLC. The equilibrium time was calculated by plotting BPA elimination versus contact time. A control experiment without N-MSW-BC was also performed under the same conditions.

IV. Synchronous degradation experiment

The synchronous degradation experiment assessed the elimination of BPA while PS-mediated oxidation and adsorption took place concurrently. N-MSW-BC (1.0 g/ L) was spiked with BPA (20.0 mg/L) and PS (10 mM) without a pre-adsorption time. Samples were

collected at intervals of 2 to 1440 min, filtered using PTFE syringe filters, quenched with sodium thiosulfate, and analyzed by HPLC (Ultimate 3000, Thermo Scientific, USA). The equilibrium time was calculated by plotting BPA elimination versus contact time. A control experiment without N-MSW-BC was also performed under the same conditions.

III. RESULTS AND DISCUSSION

A. Proximate analysis

Moisture (7.24%), volatile matter (35.97%), ash (14.97%), and fixed carbon (41.83%) content were determined. The low moisture content supports good storage stability [10]. Volatile matter reflects residual organics influencing reactivity and adsorption [11]. Ash content falls within the typical range for lignocellulosic biochar, and the mineral content may aid ion-exchange adsorption [12]. The substantial fixed carbon fraction indicates good structural stability and surface area, supporting N-MSW-BC's suitability as an adsorbent for water pollutants [11].

B. FTIR analysis of Pristine and N-doped biochar

Figure 1 shows distinctive FTIR spectral features in N-MSW-BCs relative to MSW-BC. In the pristine biochar, characteristic absorption bands were observed at 3620 cm^{-1}, 1596 cm^{-1}, 1424 cm^{-1}. The broad band at 3620 cm^{-1} is attributed to O-H stretching vibrations of hydroxyl groups associated with phenolic compounds and adsorbed water molecules. The peak at 1596 cm^{-1} corresponds to aromatic C=C skeletal vibrations and/or conjugated carbonyl groups commonly present in biochar structures. The band at 1424 cm^{-1} may be associated with aliphatic C–H bending or aromatic ring vibrations. N-MSW-BC showed enhanced broad bands to 3660-3280, which may be attributed to O-H/N-H stretching vibrations from N doping [13]. The band observed at 1594 cm^{-1} may be associated with aromatic C=C vibrations and could also involve overlapping contributions from C=N stretching and N–H bending vibrations. However, because FTIR bands may have overlapping assignments, this band alone cannot be considered definitive evidence of nitrogen-containing structures. [14]. Furthermore, the emergence of a distinct band at 1869 cm^{-1}, absent in pristine biochar, indicates the formation of nitrogen-containing surface functionalities and changes in the electronic structure of the carbon matrix during urea-assisted pyrolysis. Therefore, the FTIR results provide evidence that nitrogen doping was successfully achieved.

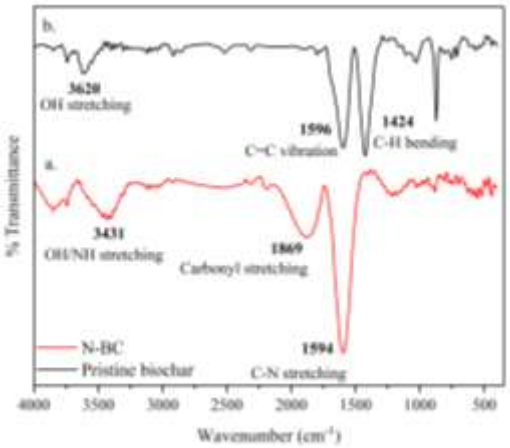


Figure 1: FTIR spectra of a) N-MSW-BC (N-doped), b) MSW-BC (pristine)

C. Zero-point charge

Using the pH drift approach, the pH_{pzc} of N-MSW-BC was determined to be 8.2 (Fig. 2), the pH at which surface charge is neutral. Below pH 8.2, the surface becomes positively charged (protonation of $–OH_2^+$/$–NH_3^+$ groups); above it, the surface becomes negatively charged (deprotonation). N-doping, which introduces functional N/O groups, is reflected in the comparatively high pH_{pzc}. Since BPA is a neutral molecule, electrostatic effects are negligible even at ambient pH (6–8); instead, π–π interactions, hydrogen bonding, and surface functional groups control adsorption.

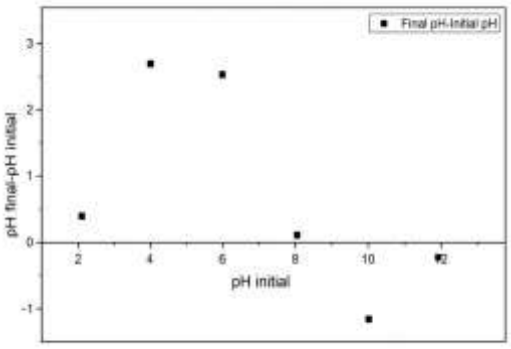


Figure 2: Zero-point charge of N-MSW-BC

D. pH edge experiment

N-MSW-BC consistently degraded BPA (~99.7%) across all measured pH values (acidic to alkaline) based on HPLC analysis, indicating pH-independent, non-electrostatic removal processes (π–π interactions, hydrophobic partitioning, hydrogen bonding, and pore-filling) rather than electrostatic attraction. Because of its resilience, N-MSW-BC can be used to treat wastewater in real-world settings without requiring pH correction.

E. Synchronous Degradation

Time-dependent degradation of BPA by N-MSW-BC (1 g/L, 20 ppm BPA) during 2-1440 min followed a triphasic trend (Fig. 3). Due to an abundance of surface-active sites and functional groups (hydroxyl, carboxyl, and nitrogen-containing moieties) that facilitate BPA absorption by hydrophobic partitioning and hydrogen bonding, clearance increased from 3.5 to 51.4% during an initial fast phase (2–60 min). A slower progressive phase (60–240 min) ensued, with a 95.6% reduction in aqueous BPA concentration, as determined by HPLC analysis. This was consistent with intraparticle diffusion into internal micro- and mesopores as exterior sites became saturated. The system approached equilibrium after 240 min, reduction in aqueous BPA concentration based on HPLC analysis only slightly increasing to 99.4, 99.7, and 99.8% at 480, 720, and 1440 min, respectively, indicating near-complete utilization of active sites; practical equilibrium was thus reached within 8–12 h, with very little additional gain (<0.5%) at 1440 min. The good agreement with the model (R^2 = 0.9955) indicates that the degradation process followed pseudo-first-order kinetics, with the reaction rate being largely dependent on the pollutant concentration under the conditions examined.

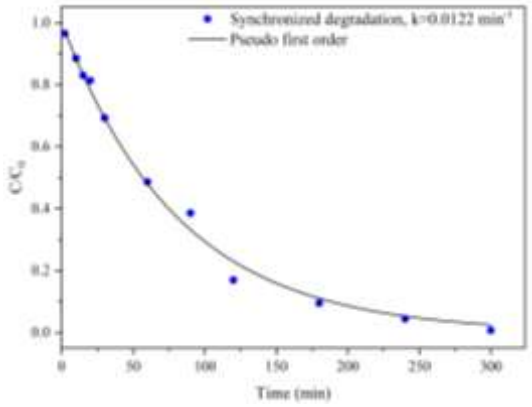


Figure 3: The fitted synchronized degradation kinetic models for BPA adsorption by N-BC at 25 °C (N-BC dosage: 1 g/L; solution volume: 250 mL; BPA concentration: 20 mg/L, PS concentration: 10 mM)

F. Adsorption kinetics

BPA adsorption proceeded quickly during the first contact period, with capacity rising sharply from 1.50 mg/g at 2 min to a maximum of 3.5 mg/g (17.5% BPA removal was achieved based on HPLC analysis.) at 90 min. It then reached an apparent equilibrium and declined slightly to 3.16 mg/g (15.5% BPA removal was achieved based on HPLC analysis.) by 1440 min. This trend is consistent with rapid initial surface mass transfer, followed by a slower approach to equilibrium, and possibly minor desorption of weakly bound BPA at longer contact times.

G. Pre-adsorption kinetics

From a mere 5.0% at 2 min to 73.9% by 120 min, and finally to 99.5–100% between 180 and 1440 min, the pre-adsorption removal was achieved, as indicated by HPLC analysis, showing a steadily increasing, eventually near-complete elimination of BPA over time. This suggests that a progressive, non-equilibrium mechanism (such as oxidative degradation) governs the entire treatment process, rather than a simple reversible adsorption step alone accounting for only a small portion of the total BPA removal observed in the system. BPA degradation follows first-order kinetics, with the degradation rate largely dependent on BPA content under the examined conditions, as indicated by the excellent fit of the pseudo-first-order kinetic model (R^2 = 0.9914).

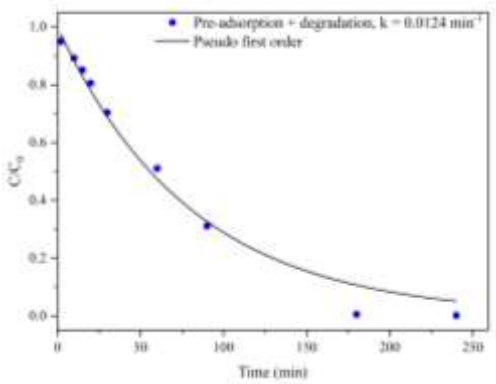


Figure : The fitted pre-adsorption degradation kinetic models for BPA adsorption by N-MSW-BC at 25 °C (N-MSW-BC dosage: 1 g/L, solution volume: 250 mL; BPA concentration: 20 mg/L, PS concentration: 10 mM)

V. CONCLUSION

In conclusion, N-MSW-BC exhibited effective BPA removal under the laboratory conditions examined, in both the synchronous adsorption–degradation and pre-adsorption-assisted PS activation configurations. Under the tested conditions, the pre-adsorption strategy achieved higher BPA removal efficiency than the synchronous approach, suggesting that pre-concentrating BPA at the biochar–water interface prior to PS activation may enhance overall removal performance. Nevertheless, the underlying degradation mechanisms remain to be fully elucidated, and the practical applicability of the N-MSW-BC/PS system warrants further investigation, particularly under more environmentally representative conditions, including real wastewater matrices, coexisting background constituents, and continuous or field-relevant operating regimes.

VI. ACKNOWLEDGMENT

The University of Sri Jayewardenepura Research Grant RC/URG/SCI/2024/14 and the Ecosphere Resilience Research Centre (ERRC), Faculty of Applied Sciences,

University of Sri Jayewardenepura are acknowledged for the financial support.

VII. REFERENCES

[1] J. Zhong, Y. Ma, S. Jiang, G. Dai, Z. Liu, and Y. Shu, "The adsorption affinity of N-doped biochar plays a crucial role in peroxydisulfate activation and bisphenol A oxidative degradation," *Environ Sci Pollut Res Int,* vol. 29, no. 59, pp. 88630-88643, Dec 2022.

[2] L. P. Lingamdinne, G. K. R. Angaru, C. A. Pal, J. R. Koduru, R. R. Karri, N. M. Mubarak, Y. Y. Chang, "Insights into kinetics, thermodynamics, and mechanisms of chemically activated sunflower stem biochar for removal of phenol and bisphenol-A from wastewater," *Sci Rep,* vol. 14, no. 1, p. 4267, Feb 21 2024.

[3] M. Kumari and M. Pulimi, "Sulfate Radical-Based Degradation of Organic Pollutants: A Review on Application of Metal-Organic Frameworks as Catalysts," *ACS Omega,* vol. 8, no. 38, pp. 34262-34280, Sep 26 2023.

[4] J. Liu, S. Jiang, D. Chen, G. Dai, D. Wei, and Y. Shu, "Activation of persulfate with biochar for degradation of bisphenol A in soil," *Chemical Engineering Journal,* vol. 381, 2020.

[5] X. Yi, X. Chen, S. Jiang, and Y. Shu, "Biochar plays multiple roles in BPA/persulfate degradation system," *Journal of Environmental Chemical Engineering,* vol. 13, no. 3, 2025.

[6] Y. Gao, W. Gao, H. Zhu, H. Chen, S. Yan, M. Zhao, H. Sun, J. Zhang, S. Zhang, "A Review on N-Doped Biochar for Oxidative Degradation of Organic Contaminants in Wastewater by Persulfate Activation," *Int J Environ Res Public Health,* vol. 19, no. 22, Nov 10 2022.

[7] R. Huang, T. Feng, S. Wu, X. Zhang, Z. Fan, Q. Yu, Y. Chen, T. Chen, "In-situ synthesis of magnetic iron-chitosan-derived biochar as an efficient persulfate activator for phenol degradation," *Environ Res,* vol. 234, p. 116604, Oct 1 2023.

[8] Y. Zhuang, S. B. Haderlein, H. V. Lutze, C. Sun, F. Fink, A. Paul, S. Spahr, "Persulfate activation by biochar for trace organic contaminant removal from urban stormwater," *Water Res,* vol. 284, p. 123921, Sep 15 2025.ss

[9] M. Dong, L. He, M. Jiang, Y. Zhu, J. Wang, W. Gustava, S. Wang, Y. Deng, X. Zhang, Z. Wang, "Biochar for the Removal of Emerging Pollutants from Aquatic Systems: A Review," vol. 20, no. 3, p. 1679, 2023.

[10] X. Yang, S. Zhang, M. Ju, and L. Liu, "Preparation and modification of biochar materials and their application in soil remediation," *Applied Sciences,* vol. 9, no. 7, p. 1365, 2019.

[11] D. Laishram, S. B. Kim, S. Y. Lee, and S. J. Park, "Advancements in Biochar as a Sustainable Adsorbent for Water Pollution Mitigation," *Advanced Science,* vol. 12, no. 19, p. 2410383, 2025.

[12] G. Zhang, L. Fang, Z. Cheng, T. Shi, X. Ma, Q. X. Li, "Highly Efficient Adsorption Characteristics and Mechanism of Nutshell Biochars for Aromatic Organophosphorus Insecticides," *Agronomy,* vol. 13, no. 2, p. 543, 2023.

[13] R. Huang, T. Feng, S. Wu, X. Zhang, Z. Yu, Y. Chen, T. Chen, "In-situ synthesis of magnetic iron-chitosan-derived biochar as an efficient persulfate activator for phenol degradation," *Environmental Research,* vol. 234, p. 116604, 2023/10/01/ 2023.

[14] Z. Liu, L. Zhao, X. He, S. Lu, H. Xiao, D. Hou, J. Ma, X. Li, F. Guo, "Enhanced adsorption of bisphenol A in using N-doped biochar from corn kernel wastes via multiple adsorption sites," *Separation and Purification Technology,* vol. 379, p. 135077, 2025/12/31/ 2025.